Updated opacities from the Opacity Project

N. R. Badnell, M. A. Bautista, K. Butler, Franck Delahaye, Claudio Mendoza, P. Palmeri, Claude J. Zeippen, M. J. Seaton

Mon. Not. R. Astron. Soc. **360,** 458–464 (2005) doi:10.1111/j.1365-2966.2005.08991.x

Updated opacities from the Opacity Project

N. R. Badnell,[1⋆] M. A. Bautista,[2] K. Butler,[3] F. Delahaye,[4,5] C. Mendoza,[2] P. Palmeri,[6]† C. J. Zeippen[5] and M. J. Seaton[7]

[1]*Department of Physics, University of Strathclyde, Glasgow G4 0NG*
[2]*Centro de Física, IVIC, PO Box 21827, Caracas 1020A, Venezuela*
[3]*Universitätssternwarte München, Scheinerstraße 1, D-81679, München, Germany*
[4]*Department of Astronomy, Ohio State University, OH 43210-1173, USA*
[5]*LUTH, Observatoire de Paris, F-92195, Meudon, France*
[6]*NASA Goddard Space Flight Center, Code 662, Greenbelt, MD 20771, USA*
[7]*Department of Physics and Astronomy, University College London, London WC1E 6BT*

Accepted 2005 March 1. Received 2004 December 16; in original form 2004 October 29

ABSTRACT

Using the code AUTOSTRUCTURE, extensive calculations of inner-shell atomic data have been made for the chemical elements He, C, N, O, Ne, Na, Mg, Al, Si, S, Ar, Ca, Cr, Mn, Fe and Ni. The results are used to obtain updated opacities from the Opacity Project (OP). A number of other improvements on earlier work have also been included.

Rosseland-mean opacities from the OP are compared with those from OPAL. Differences of 5–10 per cent occur. The OP gives the '*Z*-bump', at $\log(T) \simeq 5.2$, to be shifted to slightly higher temperatures. The opacities from the OP, as functions of temperature and density, are smoother than those from OPAL.

The accuracy of the integrations used to obtain mean opacities can depend on the frequency mesh used. Tests involving variation of the numbers of frequency points show that for typical chemical mixtures the OP integrations are numerically correct to within 0.1 per cent.

The accuracy of the interpolations used to obtain mean opacities for any required values of temperature and density depends on the temperature–density meshes used. Extensive tests show that, for all cases of practical interest, the OP interpolations give results correct to better than 1 per cent.

Prior to a number of recent investigations which have indicated a need for downward revisions in the solar abundances of oxygen and other elements, there was good agreement between properties of the Sun deduced from helioseismology and from stellar evolution models calculated using OPAL opacities. The revisions destroy that agreement. In a recent paper, Bahcall et al. argue that the agreement would be restored if opacities for the regions of the Sun with $2 \times 10^6 \lesssim T \lesssim 5 \times 10^6$ K (0.7–0.4 $R_\odot$) were larger than those given by OPAL by about 10 per cent. In the region concerned, the present results from the OP do not differ from those of OPAL by more than 2.5 per cent.

Key words: atomic processes – radiative transfer – stars: interiors.

1 INTRODUCTION

The first results for opacities from the Opacity Project (OP) were published by Seaton et al. (1994, hereafter Paper I) and were in good general agreement with those from the OPAL project (Rogers & Iglesias 1992) except for regions of high densities and temperatures.

In a more recent paper, Badnell & Seaton (2003, hereafter Paper II) confirmed a suggestion made by Iglesias & Rogers (1995) that the discrepancies in those regions were due to the omission of important inner-shell processes in the OP work. Further comparisons between OPAL results and those from the OP with inclusion of all important inner-shell processes are given by Seaton & Badnell (2004, hereafter Paper III) for the case of the six-element mix (H, He, C, O, S and Fe) of Iglesias & Rogers (1995). In Papers II and III, the required inner-shell atomic data were computed using the code AUTOSTRUCTURE (Badnell 1986, 1997). Similar computations of the required inner-shell atomic data for all cosmically abundant elements (He, C, N,

⋆E-mail: badnell@phys.strath.ac.uk
†Present address: Astrophysique et Spectroscopie, Université de Mons-Hainaut, 20 Place du Parc, B-7000 Mons, Belgium.

O, Ne, Na, Mg, Al, Si, S, Ar, Ca, Cr, Mn, Fe and Ni) have now been made. Some further improvements and updates of the OP work are also considered in the present paper.

2 OUTER-SHELL ATOMIC DATA

Most of the original OP outer-shell atomic data were computed using sophisticated R-matrix methods (see Opacity Project Team 1995, 1997). Ions are specified by nuclear charge Z and the number of 'target' electrons N: the total number of electrons in an ion is equal to $(N + 1)$. For iron ions with $N = 13$–18, the R-matrix data were supplemented by extensive data calculated by Lynas-Gray, Seaton & Storey (1995) using the code SUPERSTRUCTURE (Eissner, Jones & Nussbaumer 1974). Data for the less-abundant iron group elements, Cr, Mn and Ni, were obtained from iron data using interpolation techniques described in Paper I.

All original outer-shell atomic data were computed in Russell–Saunders coupling (LS) and allowance for fine structure was included using methods described in Paper I.

In Paper III the experiment was made of replacing all the original iron data for $N = 13$–18 by data computed in intermediate coupling using AUTOSTRUCTURE. The use of these new data did not make any major changes, which provided a good check on the earlier work, but there were some improvements due to the inclusion of intercombination lines and some improvements in photoionization cross-sections. The new intermediate-coupling iron data for iron ($N = 13$–18) are used in the present work.

As in Paper I, we use data from Kurucz (1988) for the first few ionization stages of iron-group elements.

3 INNER-SHELL ATOMIC DATA

All inner-shell atomic data were calculated using AUTOSTRUCTURE employing both LS and intermediate coupling (IC). In Paper II it was reported that, for the inner-shell work, the use of LS data and the allowance for fine structure using the methods described in Paper I did not give opacities differing significantly from those obtained using the IC atomic data. The LS inner-shell data were used in the present opacity work.

New inner-shell data have been calculated for the elements N, Ne, Na, Mg, Al, Si, Ar, Ca, Cr, Mn and Ni for $N = 1$–12. The present data were generated by working iso-electronically. Data for He, C, O, S and Fe were reported on in Paper II and were generated by working iso-nuclearly. For C, O and S, this has led to the calculation of some additional inner-shell data (see below).

The K-shell processes that were included are of the form

$$1s^q 2l^p n'l' + h\nu \rightarrow 1s^{q-1} 2l^p n'l' + e^- \tag{1}$$

for photoionization and

$$1s^q 2l^p n'l' + h\nu \rightarrow 1s^{q-1} 2l^p n'l' n''l'' \rightarrow X(N) + e^- \tag{2}$$

for photoexcitation (–autoionization), where $2l^p$ denotes $2s^s 2p^t$ with $p = s + t$. Calculations were made for $q = 1$ for $p = 0$ and $q = 2$ for $p = 0 - 7$. We used n', $n'' = 2$–5, for all allowed l', l''. The contributions from higher-n in equation (2) were obtained by matching on to the results of equation (1).

The L-shell processes that were included are

$$2l^q 3l'^p n''l'' + h\nu \rightarrow 2l^{q-1} 3l'^p n''l'' + e^- \tag{3}$$

and

$$2l^q 3l'^p n''l'' + h\nu \rightarrow 2l^{q-1} 3l'^p n''l'' n'''l''' \rightarrow X(N) + e^-, \tag{4}$$

where $3l'^p$ denotes $3s^s\ 3p^t\ 3d^u$ with $p = s + t + u$. Calculations were made for $q = 1$–7 for $p = 0$ and $q = 8$ for $p = 0$–2. We used $n', n'', n''' = 3$–6 for photoexcitation and $= 3$–5 for photoionization, for all allowed l', l'', l'''.

The M-shell processes that were included are

$$3l^q n'l' + h\nu \rightarrow 3l^{q-1} n'l' + e^- \tag{5}$$

and

$$3l^q n'l' + h\nu \rightarrow 3l^{q-1} n'l' n''l'' \rightarrow X(N) + e^-. \tag{6}$$

Calculations were made for $q = 1$ and 2 and $n', n'' = 3$–6. Calculations for $q = 3$ ($N = 13$) for Fe were made previously, and reported on in Paper II.

The ranges of p and q used in equations (1)–(6) are the same as those used in Paper II for Fe, while those used previously for C, O and S were more restrictive (but sufficient for the six-element mix). The same range of p and q has now been used for all elements. Further details of the calculations with AUTOSTRUCTURE may be found in Paper II.

The calculation using AUTOSTRUCTURE provided totals of 11 523 624 spectrum lines and 815 989 photoionization cross-sections for use in the opacity work.

4 FREQUENCY MESH

Let $u = h\nu/(kT)$ and let $\sigma(u)$ be the monochromatic opacity cross-section per atom. The Rosseland-mean cross-section is σ_R where

$$\frac{1}{\sigma_R} = \int_0^\infty \frac{1}{\sigma(u)} F(u)\,\mathrm{d}u \tag{7}$$

and

$$F(u) = [15/(4\pi^4)]u^4 \exp(-u)/[1 - \exp(-u)]^2. \tag{8}$$

The Rosseland-mean opacity per unit mass is $\kappa_R = \sigma_R/\mu$ where μ is the mean atomic weight.

The function $F(u)$ has a maximum value for $u = 3.8300\ldots$ and is small for u small and u large. It is not practicable to use a mesh in u so as to resolve all spectral-line profiles, as the number of points would be much too large. We therefore seek a mesh such that trapezoidal-rule integrations give results of acceptable accuracy. In Paper I a mesh was used with 10^4 points in the range $0.001 \leqslant u \leqslant 20$.

Equation (7) may be replaced by

$$\frac{1}{\sigma_R} = \int_{v=0}^{v_{\max}} \frac{1}{\sigma(u)}\,\mathrm{d}v \tag{9}$$

where

$$v(u) = \int_0^v F(u)\,\mathrm{d}u \tag{10}$$

and $v_{\max} = v(u \rightarrow \infty)$. From numerical integration, $v_{\max} = 1.0553\ldots$. With a given total number of integration points, *NTOT*, and constant intervals in u or v, use of equation (9) in place of equation (7) gives more points in regions giving large contributions to the integrals. It was found that the use of equation (9) gave a significant improvement in the accuracy of calculated Rosseland means.

5 ELEMENT ABUNDANCES

Results of Paper I were for a solar mix referred to as S92, based on the work of Anders & Grevesse (1989) together with some later revisions. Abundances used by Bahcall & Pinsonneault (2004) in constructing a solar model, which we refer to as BP04, are not very

Table 1. Element abundances, $A(n) = \log[N(n)]$, relative to $A(\mathrm{H}) = 12$.

Element	BP04	A04	Element	BP04	A04
H	12.00	12.00	Si	7.56	7.51
He	10.92	10.925	S	7.20	7.14
C	8.52	8.41	Ar	6.40	6.18
N	7.92	7.80	Ca	6.35	6.31
O	8.83	8.66	Cr	5.69	5.62
Ne	8.08	7.84	Mn	5.53	5.46
Na	6.32	6.17	Fe	7.50	7.44
Mg	7.58	7.55	Ni	6.25	6.18
Al	6.49	6.37			

different from those of S92 or of GN93 (Grevesse & Noels 1993) used in much of the OPAL work. However, recent work (Asplund et al. 2004, and references therein) has suggested a need for substantial revisions in solar abundances for oxygen and other elements. Dr N. Grevesse has kindly provided us with an updated table of recommended abundances, which we refer to as A04, taking account of recent work by Asplund and others. Table 1 gives, for the 17 elements considered in the present work, the abundances from BP04 and A04: BP04 gives $X = 0.7394$, $Z = 0.0170$ while A04 gives $X = 0.7403$, $Z = 0.0123$.

A detailed discussion of recent work on the solar chemical composition is given by Asplund, Grevesse & Sauval (2005).

6 CONTRIBUTIONS OF INNER-SHELL TRANSITIONS TO ROSSELAND MEANS

We use the variable

$$R = \rho/T_6^3 \tag{11}$$

introduced in the OPAL work, where ρ is mass density and $T_6 = 10^{-6} \times T$ with T in K. The behaviour of R in some stellar models is shown in figs 1 and 2 of Paper I.

Fig. 1 shows, for the S92 solar mix, $\log(\kappa_{\mathrm{R}})$ against $\log(T)$ for $\log(R) = -1$, -2, -3, -4, -5 and -6, both with and without inclusion of inner-shell transitions. It is seen that the inner-shell transitions contribute very little to the means at the lower densities, say $\log(R) \lesssim -4$. The reason is that, at a lower density, ions in a given ionization stage will have maximum abundance only at a lower temperature. At lower temperatures, features in the monochromatic opacities due to inner-shell transitions will appear at larger values of the frequency variable u corresponding to regions where the weighting function $F(u)$ in equation (7) is small.

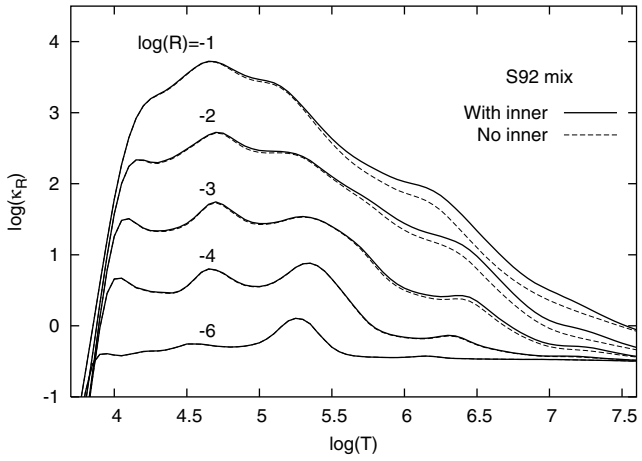

Figure 1. Rosseland-mean opacities from the OP for the S92 mix, with and without inner-shell contributions.

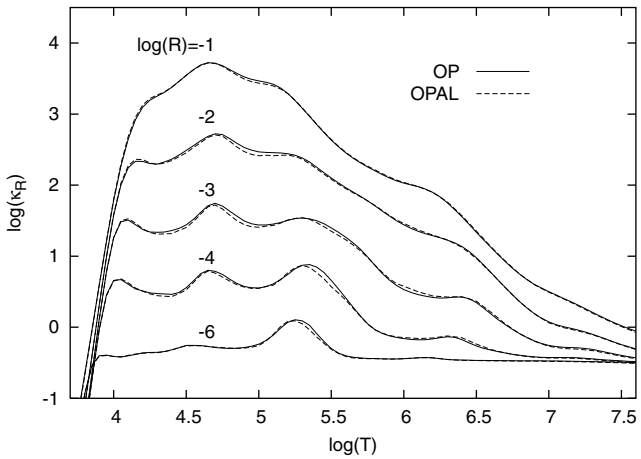

Figure 2. Rosseland-mean opacities from the OP and OPAL for the S92 mix.

7 COMPARISONS WITH OPAL

OPAL data can be obtained from the OPAL website[1] for any required composition. The basic data are given in tables of $\log(\kappa_{\mathrm{R}})$ as functions of $\log(T)$ and $\log(R)$. Codes are given for interpolations to any required values of $\log(T)$ and $\log(\rho)$ and further interpolations in X and Z.

The OP calculations of monochromatic opacities for each chemical element are made on a mesh of values of $\log(T)$ and $\log(N_{\mathrm{e}})$ where N_{e} is the electron density (the meshes used are discussed further in Section 9). A code MIXV.F reads the monochromatic opacities and calculates Rosseland means on the OP (T, N_{e}) mesh. A further code, OPFIT.F, provides interpolations to any required values of T and ρ. It includes a facility to produce tables in OPAL format. Such tables are used in comparing results from OPAL and the OP.

Fig. 2 shows $\log(\kappa_{\mathrm{R}})$ against $\log(T)$ for $\log(R) = -1$, -2, -3, -4 and -6, from both the OP and OPAL. The overall agreement is seen to be good. The feature at $\log(T) \simeq 5.2$, usually known as the 'Z-bump', is mainly due to transitions in iron ions with $N = 13$–18. It is seen that, compared to OPAL, the OP feature is shifted to slightly higher temperatures.

Use of the logarithmic scale for $\log(\kappa_{\mathrm{R}})$, as in Fig. 2, does not allow us to see the finer details of the level of agreement between the two calculations. Percentage differences (OP–OPAL) are shown in Fig. 3 for $\log(R) = -1.0$ to -2.5, and in Fig. 4 for $\log(R) = -3.0$ to -4.5. It is seen that the general level of agreement is in the region of 5–10 per cent. An excursion to larger differences at $\log(T) \simeq 5.5$, approaching 30 per cent at $\log(R) = -4.5$, is due to the differences in the high-temperature wing of the Z-bump, as shown in Fig. 2.

The differences of Figs 3 and 4 have a somewhat ragged appearance, which results from some lack of smoothness in the values of κ_{R} at the level of 1 or 2 per cent. Fig. 5 shows $\partial \log(\kappa_{\mathrm{R}})/\partial \log(T)$ at constant $\log(R)$, calculated using first differences, for $\log(R) = -2$. The data from the OP are seen to be smoother than those from

[1] See http://www-phys.llnl.gov/Research/OPAL/.

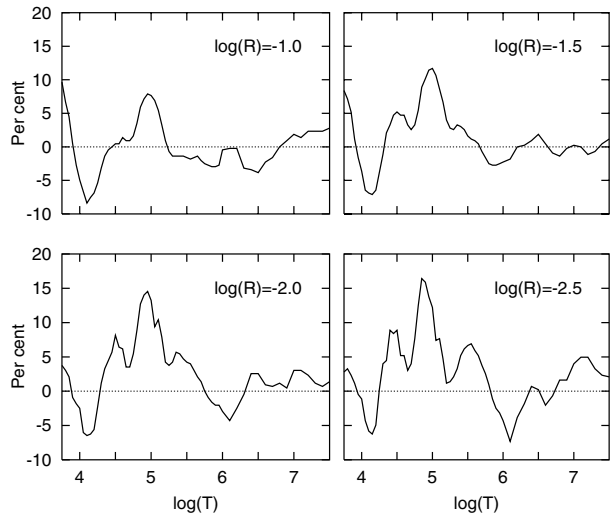

Figure 3. Percentage differences (OP–OPAL) for the S92 mix: $\log(R) = -1$ to -2.5.

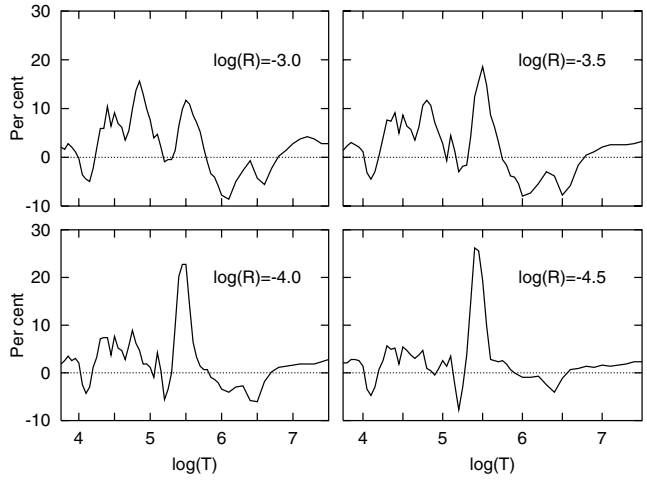

Figure 4. As Fig. 3, for $\log(R) = -3$ to -4.5.

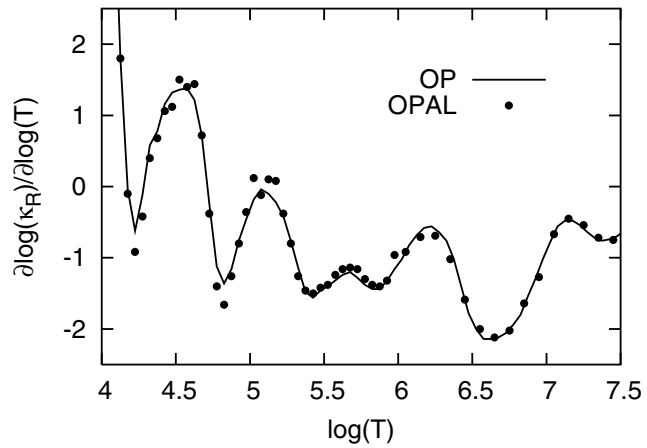

Figure 5. Values of $\partial \log(\kappa_R)/\partial \log(T)$ (at constant R) approximated using first derivatives. From the OP and OPAL for $\log(R) = -2$.

OPAL. Use of the v-mesh in the OP work (see Section 4) gives an improvement in the smoothness.

8 SOLAR RADIATIVE INTERIOR

Helioseismology provides remarkably accurate values for the depth, R_{CZ}, of the solar convection zone (CZ). With the earlier estimates of solar element abundances, such as S92 or GN93 (see Section 6), values of R_{CZ} and other data from helioseismology were found to be in good agreement with results from solar models computed using OPAL opacities. However, with the new abundances, in two recent papers it has been found necessary to increase opacities in the vicinity of R_{CZ}: by 19 per cent according to Basu & Antia (2004) and by 21 per cent according to Bahcall, Serenelli & Pinsonneault (2004). In a further detailed study of the problem, Bahcall et al. (2005) show that there are also discrepancies for the solar profiles of sound speed and density and of helium abundance. They argue that all such discrepancies would be removed if the opacities were larger than those from OPAL by about 10 per cent in the region of $2 \times 10^6 \lesssim T \lesssim 5 \times 10^6$ K(0.7–0.4 $R_\odot$).

In the solar model of Bahcall & Pinsonneault (2004), referred to as BP04, the base of the CZ is at $\log(T) \simeq 6.34$ ($r \simeq 0.715$ $R_\odot$). In the CZ, the abundances are independent of depth and the values used for the model are similar to those of the S92 mix (i.e. not taking into account recently proposed revisions). Below the CZ, $\log(T) \gtrsim 6.34$ ($r \lesssim 0.715$ $R_\odot$), abundances depend on the nuclear reactions which have taken place and vary with depth. Fig. 6 shows the Rosseland-mean opacities adopted by BP04, using OPAL data. In the CZ, the exact values of opacity are not of great importance for the calculation of a model, because in that region the temperature gradient is no longer controlled by the opacity, but comparisons of different opacity calculations are still of interest.

Fig. 7 shows percentage differences (OP–OPAL) between opacities from the OP and those used for BP04. In the region below R_{CZ}, the relative abundances of metals are assumed to be independent of depth but the mass fractions X, Y and Z are variable. We use a code MIXZ.F to obtain monochromatic opacities for the specified mixture of metals, and a code MXZ.F for variable X and Z (with $Y = 1 - X - Z$). At the lowest temperatures [say $\log(T) \leqslant 4.5$] κ_R is varying very rapidly as a function of T (see Fig. 6) and the differences

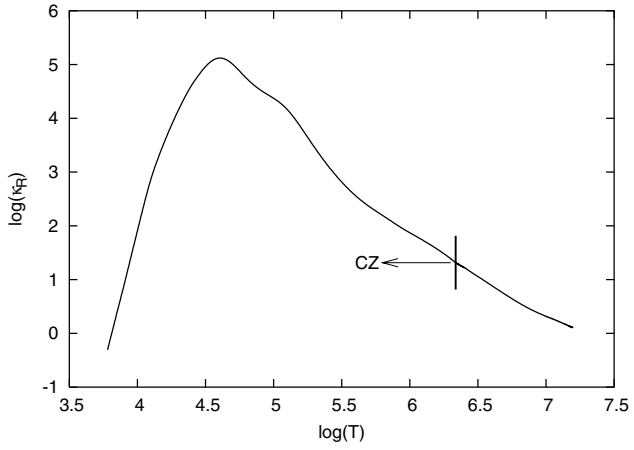

Figure 6. Rosseland-mean opacity from OPAL as used in the solar model BP04 of Bahcall & Pinsonneault (2004). The CZ is the region indicated with $\log(T) \lesssim 6.34$.

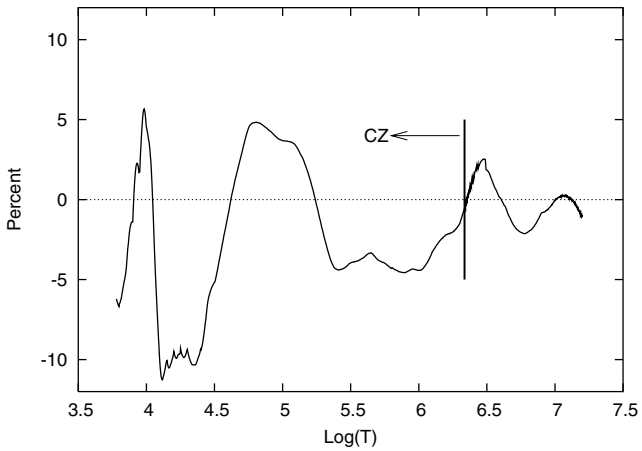

Figure 7. Percentage differences (OP–OPAL) between opacities for a solar model from Bahcall & Pinsonneault (2004). The CZ is the region with $\log(T) \lesssim 6.34$.

(OP–OPAL) are as large as 10 per cent. Throughout the rest of the CZ, the differences are never larger than about 5 per cent.

8.1 Examination of the Rosseland mean near the base of the convection zone

In the region at and below the base of the CZ, the mean opacities from the OP and OPAL do not differ by more than 2.5 per cent (see Fig. 7). In view of the current interest in the opacity in that region, we consider the results in some greater detail.

In the BP04 model, the base of the CZ is at $\log(T) = 6.338$, $\log(\rho) = -0.735$. We consider the Rosseland-mean opacity at a nearby test point on the OP (T, N_e) mesh, $\log(T) = 6.35$ and $\log(N_e) = 23.0$ giving $\log(\rho) = -0.715$ for both BP04 and A04. Fig. 8 shows $\log[\sigma(u)]$ against $u = h\nu/(kT)$ calculated using BP04 abundances. The Rosseland mean at the test point is $\kappa_R = 19.35$ cm^2 g^{-1} with BP04 and 15.29 with A04.

8.1.1 Contributing elements

The code MIXV.F used to calculate Rosseland means has a 'skip' facility: an element marked as 'skip' is included in calculating the mass density for a given electron density but its contribution to $\sigma(u)$ is omitted. Table 2 shows the result of skipping for hydrogen and helium, oxygen, and the iron-group elements. It is seen that, for all three cases, substantial contributions are skipped. We consider those three cases in greater detail.

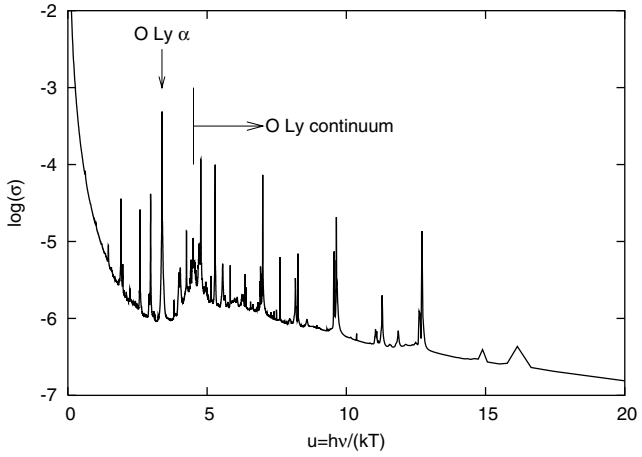

Figure 8. The monochromatic opacity for the BP04 mix at $\log(T) = 6.35$, $\log(N_e) = 23.0$. Cross-section, σ, in atomic units, πa_0^2.

Table 2. Contributions to κ_R at the test point, $\log(T) = 6.35$, $\log(N_e) = 23.0$. A04 abundances.

Skip	κ_R
None	15.29
H, He	10.51
O	10.52
Fe group	11.03

8.1.2 Contribution from hydrogen and helium

OPAL and OP results for H and He are discussed in section 7.1 of Paper III. The agreement is generally close but there is a region in the vicinity of $\log(T) \sim 6$ where OPAL has larger populations in the ground states of H and He^+, leading to larger OPAL opacities. At our test point, κ_R(OPAL) for an H/He mixture ($X \simeq 0.7$, $Y \simeq 0.3$) is about 5 per cent larger than κ_R(OP), corresponding to a difference of 2 or 3 per cent for the A04 mix.

8.1.3 Oxygen

Oxygen makes an important contribution to κ_R in the vicinity of R_{CZ} because it has a high abundance and because about half of the oxygen is in a hydrogenic state (see Table 4) and the oxygen Lyman lines and continuum come in a region where the weighting function $F(u)$ is large (see Fig. 8). The atomic data for the hydrogenic stage should be quite accurate and those for other high ionization stages should also be of good accuracy because, for a highly ionized system, the electron–nuclear potentials will be large compared with electron–electron potentials. The main uncertainties are likely to be in the level populations, as discussed in Paper III.

We do not have OPAL occupation probabilities $W(n)$ for oxygen at the test point, but we do have them for the rather similar case of carbon at $\log(T) = 6.0$, $\log(\rho) = -2.0$. From table 1 of Paper II we see that, compared with the OP, OPAL has larger occupation probabilities for more highly excited states. From that table we obtain the approximate relation

$$W_{\rm OPAL}(n) \simeq W_{\rm OP}(0.716 \times n) \qquad (12)$$

[carbon at $\log(T) = 6.0$, $\log(\rho) = -2$]

where we interpolate in n as a continuous variable. We use equation (12) to obtain estimates of $W_{\rm OPAL}(n)$ for hydrogenic oxygen. Table 3 gives populations $W(n)$ and populations $POP(n)$ for hydrogenic oxygen at the test point, from both the OP and OPAL, and Table 4 gives the corresponding ionization fractions.

The Rosseland-mean cross-sections for oxygen are $\sigma_R = 4.011 \times 10^{-4}$ atomic units (a_0^2) from the OP and 3.721×10^{-4} with our estimates of OPAL occupation probabilities. The corresponding opacities for the A04 mix are 15.75 and 15.16 cm^2 g^{-1}. The larger excited-state $W(n)$ from OPAL affect the Rosseland means in two ways. First, as noted in Paper II, they give a reduction in the ground-state population and hence a reduction in the strengths of the Lyman absorption features. Secondly, they give increases in profiles of lines

Table 3. Occupation probabilities and level populations for hydrogenic oxygen at the test point.

	OP		OPAL	
n	$W(n)$	$POP(n)$	$W(n)$	$POP(n)$
1	1.000	0.361	1.000	0.325
2	0.987	0.048	0.993	0.044
3	0.813	0.048	0.954	0.050
4	0.151	0.013	0.830	0.063
5	0.009	0.001	0.289	0.031
6	0.000	0.000	0.062	0.009
7			0.009	0.002
8			0.000	0.000

Table 4. Ionization fractions for oxygen at the test point ($N = -1$ for fully ionized, $N = 0$ for hydrogenic).

N	OP	OPAL
−1	0.415	0.374
0	0.471	0.524
1	0.109	0.098
2	0.005	0.005
3	0.001	0.000
4	0.000	

having more highly excited states and reductions in continuum absorption for dissolved lines (see appendix A of Paper I). Both effects lead to a reduction in Rosseland means.

Our value of κ_R from the OP is larger than that obtained using our estimates of W_{OPAL} for oxygen by 4 per cent.

8.1.4 Other light elements

It is shown in Paper III that, in the vicinity of R_{CZ}, carbon and sulphur have behaviours similar to that for oxygen, with σ(OP) being a few per cent larger than σ(OPAL). It can be expected that the other light elements will have a similar behaviour.

8.1.5 Iron group

It is seen from Table 2 that elements of the iron group make significant contributions to κ_R at our test point. In the vicinity of that point the dominant ionization stages for iron are oxygen-like and fluorine-like. The R-matrix atomic data for the iron group used by the OP should be of rather good accuracy. Table 5 gives values of κ_R at the test point from the OP and OPAL. The OPAL values are obtained using tables from the OPAL website and the OPAL interpolation codes XZTRIN21.F. Results are given for:

(i) A04 abundances;
(ii) A04 abundances less contributions from the iron group (number fractions are set to zero for iron-group elements, and other number fractions are unchanged except for H, for which the number fraction is increased to ensure particle conservation).

Table 5. Rosseland means at the test point.

Mixture	OP	OPAL	Per cent difference
A04	15.29	14.99	+2.0
A04 less iron group	11.03	10.63	+3.7
Difference	4.26	4.38	−2.8

It is seen that the OP contribution from the iron group is 2.8 per cent smaller than the corresponding OPAL contribution.

8.1.6 Conclusion

We recall that Bahcall et al. (2005) require κ_R to be 10 per cent larger than κ_R(OPAL) for $2 \times 10^6 \lesssim T \lesssim 5 \times 10^6$ K(0.7–0.4 $R_\odot$). In that range we find that κ_R(OP) never differs from κ_R(OPAL) by more than 2.5 per cent. The closeness of the agreement is partly fortuitous: compared with the OP, OPAL has larger contributions from H and He and from the iron group, but smaller contributions from oxygen. However, an increase to 10 per cent larger than OPAL in the region $2 \times 10^6 \lesssim T \lesssim 5 \times 10^6$ K does not appear to be very plausible.

9 CHECKS ON ACCURACIES OF INTERPOLATIONS AND OF FREQUENCY MESH

Temperature and density indices I and J are defined by

$$\log(T) = 0.025\, I, \qquad \log(N_e) = 0.25\, J. \tag{13}$$

Four meshes are used:

(i) fine mesh, 'f', $\Delta I = \Delta J = 1$;
(ii) medium mesh, 'm', $\Delta I = \Delta J = 2$;
(iii) coarse mesh, 'c', $\Delta I = \Delta J = 4$;
(iv) very coarse mesh, 'C', $\Delta I = \Delta J = 8$.

The number of frequency points, equally spaced in the variable v (see Section 4), is taken to be equal to *NTOT*. Normal OP production work is carried out using the 'm' mesh with even values of I and J, and $NTOT = 10\,000$. OPAL production work is carried out with 10 000 equally spaced points in the variable $u = h\nu/(kT)$, $0.002 \leqslant u \leqslant 20$. Checks on the accuracies of our integrations over frequency and interpolations in T and ρ were made for a solar mix.

First, check calculations were made using the 'C' mesh with $NTOT = 10\,000$ and 20 000. It was found that use of the finer frequency mesh ($NTOT = 20\,000$) never led to a change in the Rosseland mean of more than 0.1 per cent.

Then, 'C' calculations were made for odd values of I and J, so that none of the 'C' mesh points coincided with 'm' mesh points. Using values of Rosseland means for the 'm' points, interpolations to the 'C' points were made using the code OPFIT.F (Seaton 1993). For $\log(T) \geqslant 3.73$ and $\log(R) \leqslant -1.0$, all differences are less than 0.6 per cent. Larger differences occur only in two regions: small $\log(T)$, where κ_R is varying rapidly as a function of T (see Fig. 1) – the worst case is 1.6 per cent at $[\log(T) = 3.525, \log(R) = -7.2]$; and large $\log(R)$, close to the upper boundary for OPFIT interpolations – worst cases are 3.1 per cent at $[\log(T) = 6.525, \log(R) = -0.530]$ and 5.8 per cent at $[\log(T) = 7.25, \log(R) = -0.531]$.

Bahcall et al. (2004) report that the use of OPAL opacities and different interpolation schemes yield opacity values in the solar-centre region differing by as much as 4 per cent. In view of the importance of obtaining accurate opacities for that region, we have made further checks. For $6.0 \leqslant \log(T) \leqslant 8.0$ we have made 'm' mesh calculations with *NTOT* equal to both 10 000 and 30 000. For all densities considered in the OP work [$\log(N_e) = 15.5$–23.5 for $\log(T) = 6.0$, $\log(N_e) = 22.0$–29.5 for $\log(T) = 8.0$] we find the largest differences in single-element Rosseland means, for

NTOT = 10 000 and 30 000, to be about 4 per cent. Such comparatively large differences occur only for cases with deep minima in the monochromatic opacities. For typical mixtures, such minima become filled in by contributions from other elements, and the sensitivities to *NTOT* become much smaller. For a solar-type mix, $6.0 \leqslant \log(T) \leqslant 8.0$ and all densities, the differences between $\kappa_{\rm R}$ for *NTOT* = 10 000 and 30 000 are never larger than 0.1 per cent.

As a further check on interpolations we have made calculations using both the 'm' and 'f' meshes with *NTOT* = 10 000. We used OPFIT.F to make calculations for a model with a fine mesh in $\log(T)$ and densities so as to give $\log(R) = -1.75$, roughly corresponding to a solar-centre model. For $6.2 \leqslant \log(T) \leqslant 7.5$, values of $\kappa_{\rm R}$ from the 'm' and 'f' calculations never differ by more than 0.4 per cent; for the vicinity of the base of the CZ, they never differ by more than 0.1 per cent.

10 DATA ARCHIVES

10.1 Outer-shell atomic data

The OP outer-shell atomic data are archived in TOPbase, which is part of the OP archive at the Centre de Données de Strasbourg (CDS).[2] The original version of TOPbase is described by Cunto et al. (1993).

10.2 Atomic data from AUTOSTRUCTURE

Both inner- and outer-shell data from AUTOSTRUCTURE have been archived according to the Atomic Data and Analysis Structure (ADAS) ADF38 and ADF39 data formats (Summers 2003). We have included LS and IC final-state resolved photoexcitation–autoionization and photoionization data, summed over final channel angular momenta for both inner and outer shells. This will enable the data to be used in the future for other purposes such as the collisional–radiative modelling of photoionized plasmas. Further details of the data archival may be found in Paper II.

10.3 Monochromatic opacities and computer codes

Codes for the calculation of Rosseland-mean opacities and radiative accelerations for any chemical mixtures, temperatures and densities are described by Seaton (2005). A TAR file containing the codes and all required monochromatic opacities is available for download from the TOPbase website at the CDS. Because the file size is a little under 700 Mb, it is also available on a CD.[3]

10.4 OPserver

Rosseland-mean opacities and their derivatives can also be computed on-line for any required chemical mixture using the OPserver at the Ohio Supercomputer Center, Columbus, OH, USA (Mendoza et al., in preparation). It can be accessed via the TOPbase website at the CDS.

11 SUMMARY

The OP opacities have been updated by inclusion of all contributing inner-shell processes and some further refinements have been made.

Comparisons with OPAL show agreement generally to within 5–10 per cent.

Using earlier estimates of metal abundances, good agreement was obtained between computed solar models and results obtained from helioseismology for $R_{\rm CZ}$ and other data. With recent downward revisions in metal abundances, that agreement is destroyed. It is shown by Bahcall et al. (2005) that agreement would be restored if opacities in the region just below the base of the CZ, $2 \times 10^6 \lesssim T \lesssim 5 \times 10^6$ K (0.7–0.4 $R_\odot$), were 10 per cent larger than those from OPAL. In that region we find $\kappa_{\rm R}$(OP) never to be larger than $\kappa_{\rm R}$(OPAL) by more than 2.5 per cent. Results for opacities in the region near the base of the CZ have been discussed in some detail.

Studies have been made of the accuracies of the OP integrations over frequency, used to obtain Rosseland means, and of the OP procedures used for interpolations in temperature and density. It is concluded that the OP Rosseland means should be numerically correct to within 1 per cent or better.

ACKNOWLEDGMENTS

We thank Dr N. Grevesse for providing the table of abundances which we refer to as A04, and Dr A. M. Serenelli for providing the table of abundances for BP04. We thank Dr J. N. Bahcall for advice and comments. FD is grateful to the INSU/CNRS for support during visits to Meudon.

REFERENCES

Anders E., Grevesse N., 1989, Geochim. Cosmochim. Acta., 53, 197
Asplund M., Grevesse N., Sauval A. J., Allende Prieto C., Kiselman D., 2004, A&A, 417, 751
Asplund M., Grevesse N., Sauval A. J., 2005, in Bash F. N., Barnes T. G., eds, ASP Conf. Ser. Vol. 336, Cosmic Abundances as Records of Stellar Evolution and Nucleosynthesis. Astron. Soc. Pac., San Francisco, in press (astro-ph/0410214)
Badnell N. R., 1986, J. Phys. B, 19, 3827
Badnell N. R., 1997, J. Phys. B, 30, 1
Badnell N. R., Seaton M. J., 2003, J. Phys. B, 36, 4367 (Paper II)
Bahcall J. N., Pinsonneault M. H., 2004, Phys. Rev. Lett., 92, 121301
Bahcall J. N., Serenelli A. M., Pinsonneault M., 2004, ApJ, 614, 464
Bahcall J. N., Basu S., Pinsonneault M., Serenelli A. M., 2005, ApJ, 618, 1049
Basu S., Antia H. M., 2004, ApJ, 606, L85
Cunto W., Mendoza C., Ochsenbein F., Zeippen C. J., 1993, A&A, 275, L5
Eissner W., Jones M., Nussbaumer H., 1974, Comput. Phys. Commun., 8, 270
Grevesse N., Noels A., 1993, in Pratzo M., Vangioni-Flam E., Casse M., eds, Origin and Evolution of the Elements. Cambridge Univ. Press, Cambridge, p. 15
Iglesias C. A., Rogers F. J., 1995, ApJ, 443, 460
Kurucz R. L., 1988, in McNally D., ed., Trans. IAU, XXB. Kluwer, Dordrecht, p. 168
Lynas-Gray A. E., Seaton M. J., Storey P. J., 1995, J. Phys. B, 28, 2817
Opacity Project Team, 1995, The Opacity Project Vol. 1. IOP Publishing, Bristol
Opacity Project Team, 1997, The Opacity Project Vol. 2. IOP Publishing, Bristol
Rogers F. J., Iglesias C. A., 1992, ApJS, 79, 507
Seaton M. J., 1993, MNRAS, 265, L25
Seaton M. J., 2005, MNRAS, in press (astro-ph/0411010)
Seaton M. J., Badnell N. R., 2004, MNRAS, 354, 457 (Paper III)
Seaton M. J., Yu Yan, Mihalas D., Pradhan A. K., 1994, MNRAS, 266, 805 (Paper I)
Summers H. P., 2003, ADAS User Manual (Version 2.6) http://adas.phys.strath.ac.uk

[2] See http://cdsweb.u-strasbg.fr/topbase.
[3] Requests to Claude.Zeippen@obspm.fr.

This paper has been typeset from a TEX/LATEX file prepared by the author.